Eur. Phys. J. E (2023) 46:124
https://doi.org/10.1140/epje/s10189-023-00377-5

THE EUROPEAN PHYSICAL JOURNAL E

Regular Article – Living Systems

The Soret coefficient of human low-density lipoprotein in solution: a thermophilic behavior

Luciene Oliveira Machado[a], Dennys Reis, and Antônio Martins Figueiredo Neto

Institute of Physics, University of São Paulo, São Paulo, Brazil

Received 3 June 2023 / Accepted 10 November 2023 / Published online 7 December 2023

Abstract Thermodiffusion, or Soret effect, is the physical phenomenon of matter gradients originated by the migration of chemical species induced by thermal gradients. Thermodiffusion has been widely applied in the study of colloidal suspensions. In this study, we investigate the termodiffusion behavior of low-density lipoprotein (LDL) particles, by the Soret coefficient measurement. It is a new approach to studies of plasma lipoproteins. The experimental work was based on thermal- and Soret-lens effects. These effects were induced by laser irradiation of the samples, at two different time scales, in a Z-scan setup. LDL samples were analyzed under physiological conditions, notedly, ionic strength and pH, and at different temperatures. Temperature dependence of Soret coefficient showed a slight decrease in the absolute value of this coefficient, as a function of temperature increasing. However, its sign does not change at the temperatures investigated (15, 22.5 and 37.5 °C). The results show that LDL particles exhibit thermophilic behavior. The origin of this thermophilic behavior is not yet completely understood. We discuss some aspects that can be related with the Soret effect in LDL samples.

1 Introduction

Thermodiffusion, also called Soret effect [1], is the physical phenomenon of mass transport originated by the migration of chemical species, as ions or particles, induced by thermal gradients. Temperature gradients are originated by non-homogeneous distribution of heat in solutions, leading to the formation of hot and cold regions in the medium. The particles can migrate to these hot or cold regions exposing thermophilic or thermophobic behaviors, respectively. The quantitative assessment of the thermodiffusive phenomenon is made by measuring the Soret coefficient (S_T) that relates the mass concentration gradient to the temperature gradient. Positive Soret coefficient is associated to thermophobic migration of particles, while negative coefficient is associated with thermophilic behavior [2].

The physical bases of the Soret effect in colloidal solution are not completely understood; nevertheless, many studies had showed the dependence of the S_T with physical parameters as surface charge of particles, ionic strength and pH of the solutions [3–5]. Beyond of the thermal gradient, the temperatures of hot and cold regions of the system have influence mass migration [3, 6]. As result, S_T can exhibit variations in magnitude and sign, depending on the equilibrium temperature. In some colloidal solutions, a sign inversion, from negative S_T to positive, occurs in response to increasing temperature [3, 6]. The study of the temperature dependence of S_T ($S_T(T)$) has been also helpful to clarified some aspects of thermodiffusion in many systems [7–9]. The behavior of $S_T(T)$ has been associated to hydrophilicity or hydrophobicity nature of the particles and their capacity to alter the hydrogen bonding of water molecules [10, 11].

In this work, we studied the thermodiffusion of human low-density lipoprotein (LDL) particles. LDL is a cholesterol carrier in animal organisms, and its role in the development of cardiovascular diseases, such as atherosclerosis, is widely accepted. Although known, the mechanisms that lead to atherogenic character of LDL are not yet fully elucidated. A more extensive understanding of the composition, structure and behavior of LDL in physiological environments may contribute to the knowledge about atherogenic role of this lipoprotein.

LDL particles are composed of a hydrophobic lipid core, in which are triglycerides and cholesteryl esters. This core is surrounding by a hydrophilic monolayer constituted of phospholipids, unesterified cholesterol and a single apolipoprotein (ApoB-100) [12–14]. The composition of LDL also includes some lipophilic antioxidants, such as tocopherols and carotenoids [13], that are essential for the protection of lipoprotein against oxidative processes. For LDL particles, diameter is suggest a range of 18–25 nm [12].

[a] e-mail: lu_machado@usp.br (corresponding author)

An interesting aspect concerning the LDL particles is the thermodiffusion. Since temperature gradients can be established in the bloodstream, as result of conditions as hyperthermia or hypothermia, thermodiffusion may have effects in the development of the CVD due to the Soret effect on the LDL particles. Hyperthermia is a process used in various treatments for different pathologies [15, 16]. In a theoretical study of LDL thermodiffusion in arterial wall, under hyperthermia conditions, Chung and Vafai [15] investigated the Soret effect role in LDL transport. A typical positive value of Soret coefficient ($S_T > 0$) of about 0.01 was adopted. A lower value of $S_T = 0.005$ was also employed based on an expected decrease in S_T due to the large dimension of LDL [15]. The study describes an LDL particle accumulation inside the arterial wall as result of the thermal gradient induced by hyperthermia. Despite the existence of theoretical investigations on LDL migration [15–18], experimental studies of the Soret effect in LDL solutions remain absent in the literature.

For charged nanoparticles in aqueous solutions, due to the presence of the electric double layer generated by their surface charges, the temperature dependence of the capacitive energy around the nanoparticles was shown to be related to particles thermodiffusion [19, 20]. In addition, ions dispersed in the solutions also respond to the temperature gradient and can create a thermoelectric field, driving particles either to cold or hot regions [19, 21]. The hydrophobicity has been also related to thermodiffusion behavior in colloidal solutions, including the temperature dependence of S_T [10, 11]. These physical mechanisms, or the combination of them, suggest that the LDL particles dispersed in blood plasma can migrate in the presence of a thermal gradient. However, the impossibility of an individual analysis of these contributions makes it extremely difficult to determine precisely the physical bases that originate the termoddifusion in the LDL samples. Consequently, a correct theoretical prediction of the termodiffusion behavior on LDL particles is still missing.

In our experimental approach, we present an application of the generalized thermal-lens model (GTLM) [22], employed to measure the different lens (electronic, thermal and matter), by ZS experiments, to study the thermodiffusion of human LDL particles, under physiological conditions (e.g., pH and ionic strength). The technique was employed to measure the amplitude and sign of the Soret coefficient of LDL particles. The temperature dependence of LDL S_T was also analyzed.

2 Theoretical background

The total mass flux ($\overrightarrow{J_M}$) in a colloidal solution can be written considering the contributions of thermal and matter gradients [2, 23],

$$\overrightarrow{J_M} = -D_M \vec{\nabla} c - c D_T \vec{\nabla} T \tag{1}$$

where D_M is the mass diffusion coefficient, D_T is the thermal diffusion coefficient, $\vec{\nabla} T$ and $\vec{\nabla} c$ are, respectively, temperature and mass gradients and c is the mass/volume concentration of particles in the solution. At the steady state of mass migration, there is a coupling between thermal and mass transfers. Under this condition, Soret coefficient is defined as follows [2, 23]:

$$S_T = \frac{D_T}{D_M} = \frac{-1}{c}\frac{\Delta c}{\Delta T} \tag{2}$$

In complex fluids, the Soret effect depends on different mechanisms and parameters [22, 24] making a theoretical prediction of their individual contributions difficult. In this context, the main aim of the present study was to develop an experimental approach to determine the Soret coefficient (S_T) of LDL particles.

2.1 The Z-scan technique

The optical experiment employed to measure the Soret coefficient is based in the Z-scan technique [25]. In this technique, a sample is illuminated by a sequence of light pulses (pulse duration Δt) and moved along a Gaussian laser beam direction (z-axis). The transmittance is measured as a function of experimental time and z-position of the sample. The incident beam is focused by a converging lens, resulting in beam waist (with a beam radius w_0) formation. Z-scan technique is used to study the phenomenon of lens behavior of the samples. Depending on the characteristic lens formed, and the sample position with respect to the focus location, the transmitted beam may be focused or defocused in the detector position. This leads to variations in the optical transmittance measured by the detector. The GTLM [22] proposes that, depending on Δt and sample's light absorption characteristic, different physical phenomena can be assessed. In the case of the LDL, light pulses of $\Delta t = 40$ms lead to the formation of the thermal lens, whereas $\Delta t = 20$s leads the formation of the matter lens (thermodiffusion).

The laser beam employed has a radial Gaussian profile in the plane of the sample, imposing a radial temperature gradient across the sample. This thermal gradient imposes a radial index refraction gradient in the sample. As stressed before, the thermal or Soret lens are formed, depending on Δt. The normalized transmittance is written as [22, 26] follows:

$$T_N^{-1}(z, t) = 1 - 2\gamma\frac{z_0}{f(t)} + \left(1+\gamma^2\right)\left[\frac{z_0}{f(t)}\right]^2 \tag{3}$$

where $f(t)$ is the focal length of the lens formed, $z_0 = \frac{\pi {w_0}^2}{\lambda}$ is the Rayleigh parameter and $\gamma = z/z_0$ is the relative position of sample [22, 26].

Assuming the parabolic approximation, the increment of temperature in the sample, as a function of the

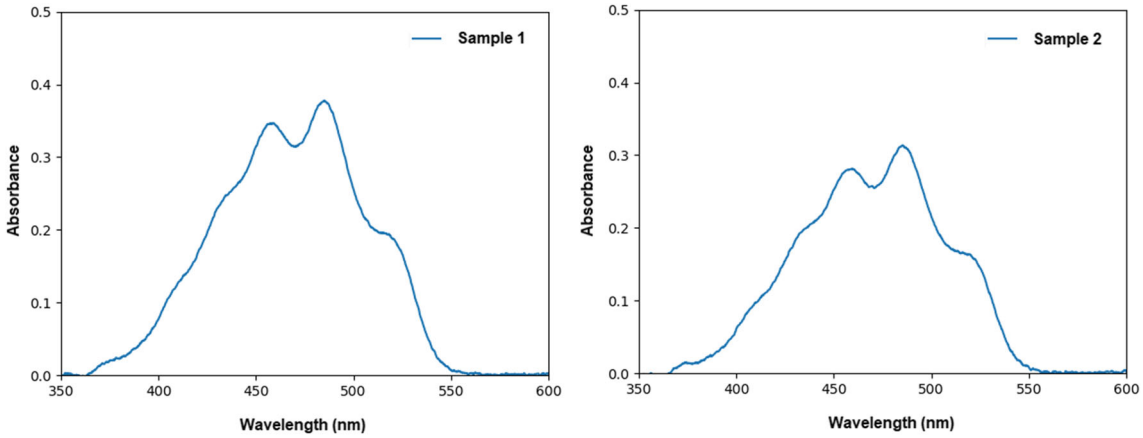

Fig. 1 LDL absorbance spectra in the wavelength range from 350 to 600 nm, allowing to evaluate the samples levels of carotenoid antioxidants

time (t) and the radial distance (r), is given by [26]:

$$\Delta T(r,\,t) = \frac{0.06\alpha P}{\pi k_T}\left[\ln\left(1+\frac{2t}{t_{\mathrm{TL}}}\right) - 2\left(\frac{r}{w}\right)^2 \frac{2t}{2t+t_{\mathrm{TL}}}\right] \tag{4}$$

where α is the optical absorption coefficient, P is the incident power, k_T is the sample thermal conductivity and t_{TL} is the characteristic heat diffusion time. The inverse focal distance of the thermal lens ($1/f_{\mathrm{TL}}$) depends on the thermo-optical coefficient $\mathrm{d}n/\mathrm{d}T$, where n is the index of refraction, is written as [22, 26] follows:

$$\frac{1}{f_{TL}} = -l\left(\frac{\mathrm{d}n}{\mathrm{d}T}\right)\frac{\mathrm{d}^2\Delta T(r,\,t)}{\mathrm{d}r^2} \tag{5}$$

The normalized transmittance, as a function of time and sample position, $T_N(z,\,t)$, is given by [26]:

$$T_N^{-1}(z,\,t) = \left(\frac{T(z,\,t)}{T(z,\,t_0)}\right)^{-1} = 1 - 2\gamma\frac{2\theta_{\mathrm{TL}}t}{(1+\gamma^2)\,2t+t_{\mathrm{TL}}} + \left(1+\gamma^2\right)\left[\frac{2\theta_{\mathrm{TL}}t}{(1+\gamma^2)\,2t+t_{\mathrm{TL}}}\right]^2 \tag{6}$$

where the thermal-lens amplitude is defined by $\theta_{\mathrm{TL}} = \frac{0.24\alpha Pl}{\lambda k_T}\left(\frac{\mathrm{d}n}{\mathrm{d}T}\right)$.

A similar mathematical development can be done to obtain the expression for the matter lens. The increment of concentration, $\Delta c(r,\,t) = -cS_T\Delta T$ [6, 22], is written as follows:

$$\Delta c\,(r,\,t) = \frac{-0.06\alpha PcS_T}{\pi k_T}\left[\ln\left(1+\frac{2t}{t_{SL}}\right) - 2\left(\frac{r}{w}\right)^2\frac{2t}{2t+t_{SL}}\right]^2 \tag{7}$$

The inverse of the focal distance associated to the matter lens ($1/f_{SL}$) is defined as follows [22]:

$$\frac{1}{f_{SL}} = -l\left(\frac{\mathrm{d}n}{\mathrm{d}c}\right)\frac{\mathrm{d}^2\Delta c(r,\,t)}{\mathrm{d}r^2} \tag{8}$$

From Eq. (3), the normalized transmittance, $T_N(z,\,t)$, is given by

$$T_N^{-1}(z,\,t) = \left(\frac{T(z,\,t)}{T(z,\,t_0)}\right)^{-1} = 1 - 2\gamma\frac{2\theta_{SL}t}{(1+\gamma^2)\,2t+t_{SL}} + \left(1+\gamma^2\right)\left[\frac{2\theta_{SL}t}{(1+\gamma^2)\,2t+t_{SL}}\right]^2 \tag{9}$$

where θ_{SL} is the Soret-lens amplitude [19], written as follows:

$$\theta_{SL} = -\theta_{TL}cS_T\left(\frac{\mathrm{d}n}{\mathrm{d}T}\right)^{-1}\left(\frac{\mathrm{d}n}{\mathrm{d}c}\right) \tag{10}$$

3 Materials and methods

3.1 Sample preparation

Human plasma from healthy donors was obtained from COLSAN (Beneficent Blood Collection Association—São Paulo, Brazil). Protease inhibitors and antioxidant were added to the plasma [27, 28]. LDL particles were isolated by sequential ultracentrifugation [29]. In this work, this preparative method was carried out using an ultracentrifuge equipped with a fixed-angle rotor (Hitachi®Himac CP 70MX, Tokyo, Japan) at 10^5 g and 4 °C for 20 h. Potassium bromated (KBr) was added to adjust the LDL density cut-off point (1.063 g/mL) [28]. LDL was dialyzed against

phosphate-saline solution (NaCl 150 mM, Na_2HPO_4 10 mM, pH 7,4 with EDTA 10 mM) to remove the KBr. The dialysis process efficiency was monitored by pH and conductivity measurement. Protease inhibitors were added to the LDL samples. Samples were filtered with a micrometric size pore filter. LDL total protein concentrations were determined using BCA Protein Assay Kit (Pierce®) with bovine serum albumin (BSA), and the absorbance was measured at 562 nm, by a microplate reader (800 TS, BioTek).

LDL samples were characterized by dynamic light scattering (DLS) in order to verify the average particle diameter and the size distribution of the particles in the samples (Supplemental Material). The samples were used immediately after the preparation, to avoid oxidation or particle's agglomeration effects. For this reason, an LDL sample from a new preparation batch was used in each set of experiments. Different LDL samples were named by a numerical index.

3.2 UV–Vis spectroscopy

The sample absorption coefficient α was determined from the absorbance measurement (A) at 532 nm, $\alpha = A\ln 10/b$, where $b = 10$mm is the path length. The absorbance spectra were obtained from measurements of the extinction, removing the Rayleigh-scattering contribution. The extinction spectra were measured in a UV–Vis spectrometer (USB4000, Ocean Optics®) in the wavelength range from 200 to 800 nm. The sample was placed in a quartz cuvette [27, 28].

3.3 Optical coefficients

The linear dependence of refractive index (n) with temperature (T) and LDL samples concentration (c) was used to determine the optical coefficients $\mathrm{d}n/\mathrm{d}T$ and $\mathrm{d}n/\mathrm{d}c$, respectively. Refractive index measurements were performed in a refractometer (ATAGO 5000i).

3.4 Z-scan

The Z-scan setup is composed by a Gaussian laser beam, wavelength of $\lambda = 532$ nm (Verdi V10, Coherent). The beam is focused by a converging lens, resulting in a beam waist in the focus position (w_0). An iris is positioned in front of the detector to limit the light intensity detected. Time evolution of light intensities is acquired by an oscilloscope, connected to the detector. Acquisition software records the data from oscilloscope. Samples were placed inside a quartz cuvette, with 200 μm of optical path length (Hellma Q170-700). The laser power was set to 0.15 W, and the temperature was set at 22.5 ± 0.1 °C.

To generate the thermal lens, pulses of $\Delta t = 40$ms of irradiation time were employed, followed by a time interval of 1 s without light. In the Soret-lens experiments, pulses of $\Delta t = 20$s of irradiation time were employed, followed by a time interval of 120 s without light.

Table 1 P, α and c are the laser light incident power, the absorption coefficient and sample concentration, respectively

Native LDL	P(W)	$\alpha(\mathrm{m}^{-1})$	c(mg/mL)	θ_{TL}	θ_{SL}	$\mathrm{d}n/\mathrm{d}T(\mathrm{K}^{-1})$	$\mathrm{d}n/\mathrm{d}c(\mathrm{mg/mL})^{-1}$	S_T (K^{-1})
Sample 1	0.15	23.7	1.3	− 0.034 ± 0.001	0.014 ± 0.002	− 1.12×10^{-4}	1.15×10^{-3}	− 0.031 ± 0.005
Sample 2	0.15	21.6	1.0	− 0.030 ± 0.001	0.021 ± 0.002	− 1.11×10^{-4}	1.11×10^{-3}	− 0.070 ± 0.007

θ_{TL}, θ_{SL} and S_T are the amplitude of the thermal and matter lenses and the Soret coefficient, respectively. $\mathrm{d}n/\mathrm{d}T$ is the thermal coefficient, and $\mathrm{d}n/\mathrm{d}c$ is the variation of the refractive index as a function of the sample concentration

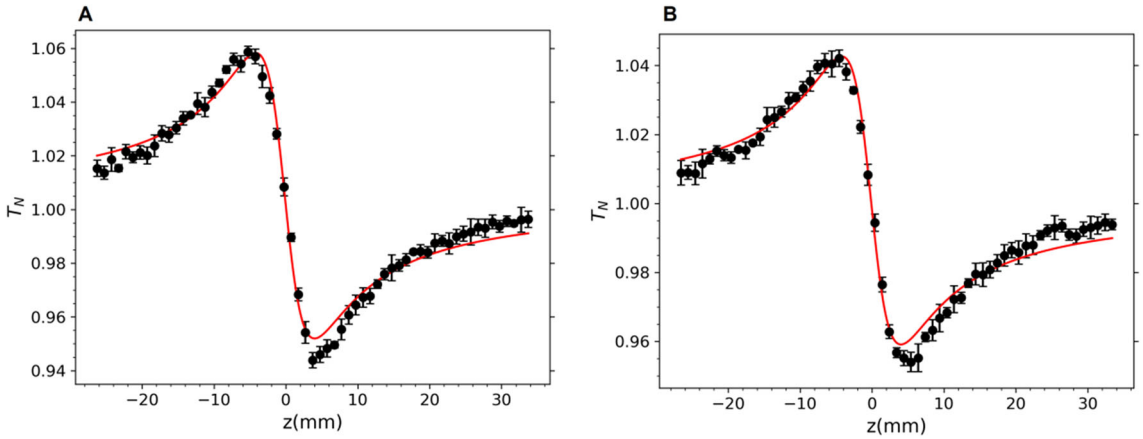

Fig. 2 Z-scan thermal-lens results for the LDL samples 1 (**A**) and 2 (**B**). Symbols represent experimental data, and lines are the theoretical fittings (Eq. 11)

Experimental data of the normalized transmittance as a function of the z-position of the sample were fitted with the time-independent Eq. (11):

$$T_N^{-1}(z) = \left(\frac{T_N(z,t)}{T_N(z,t_0)}\right)^{-1} = 1 - 2\gamma\frac{\theta}{(1+\gamma^2)} + (1+\gamma^2)\left[\frac{\theta}{(1+\gamma^2)}\right]^2 \quad (11)$$

4 Results and discussion

4.1 Linear light absorbance

The absorption spectra, for samples 1 and 2, are shown in Fig. 1.

These results show characteristic absorbance spectra of LDL [27, 28] in which the heterogeneous constitution of these particles gives different contributions. We focus on the wavelength range from 350 to 600 nm, where the maximum light absorption of carotenoid antioxidants (at $\lambda \approx 440$–480 nm) can be observed. This range also shows the samples absorbance at $\lambda = 532$ nm, the laser wavelength used in our experiments. From the absorbance values at 532 nm, the optical absorption coefficient (α) of the samples was determined (Table 1).

Light absorbance in a medium, resulting in a non-homogeneous heat distribution, is the principle of the lens behavior of the samples in a Z-scan experiment. As shown, the LDL samples have an absorbance at $\lambda = 532$ nm, the laser wavelength used in our experiments. This absorbance and the inhomogeneous distribution of heat in the samples make possible the thermal- and mass-lens experiments, the results of which are present below.

4.2 Thermal lens

In the thermal-lens experiments, LDL samples were irradiated with light pulses $\Delta t = 40$ms, in the ZS setup. The characteristic peak-to-valley behavior, for both samples 1 and 2, is shown in Fig. 2.

As the matter-lens experiment takes a long time (about 10 h), we repeated the measurement of the thermal-lens amplitude, after the matter-lens experiment. The amplitude of the thermal lens was shown to be reduced, with respect to the first measurement, probably due to the light irradiation time of the sample. To calculate the Soret coefficient (in the following), we used a mean value from both measured thermal-lens amplitudes.

The mean values of θ_{TL} for both samples are negative, corresponding to negative thermo-optical coefficient. These values are about the same (see Table 1), indicating that both LDL samples, from different plasmas, presented equivalent thermal behavior.

4.3 Matter-lens and the Soret coefficient

In the matter-lens experiments, LDL samples were irradiated with light pulses $\Delta t = 20$s, in the ZS setup. The valley-to-peak behavior, for both samples 1 and 2, is shown in Fig. 3. Interestingly, this characteristic behavior valley-to-peak curves differ from that of the thermal lens, that is, peak-to-valley.

The experimental matter-lens curves were also fitted with Eq. (11). The best fittings are shown in Fig. 3, and, from these fits, the matter-lens amplitudes (θ_{SL}) were obtained (Table 1). The Soret coefficient was determined (Eq. 10) for both samples and is presented in Table 1.

The optical coefficients $\mathrm{d}n/\mathrm{d}T$ and $\mathrm{d}n/\mathrm{d}c$ (Table 1) were determined by the dependence of the refractive index (n) on the temperature and sample concentration, respectively, as described in methodology. Figure 4 shows a typical result to the linear dependence between these parameters.

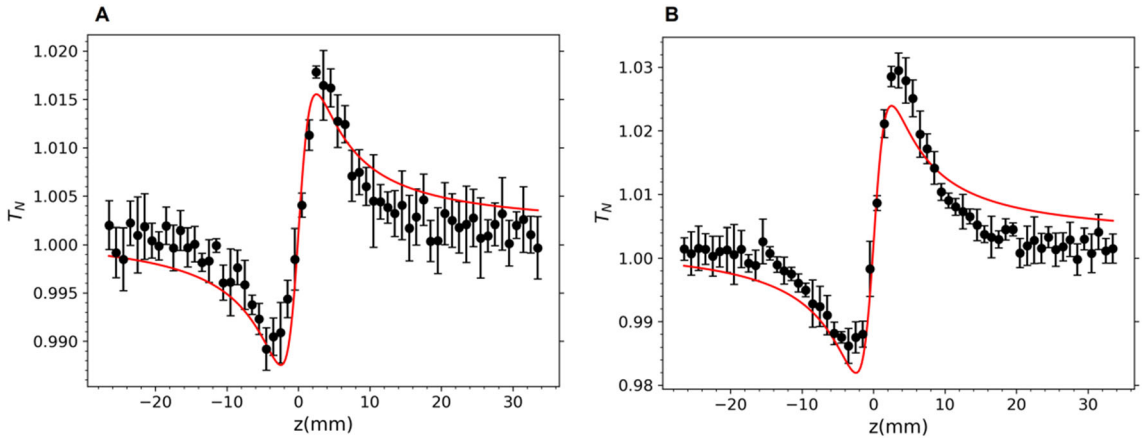

Fig. 3 Z-scan matter-lens results for the LDL samples 1 (**A**) and 2 (**B**). Symbols represent experimental data, and lines are the theoretical fittings (Eq. 11)

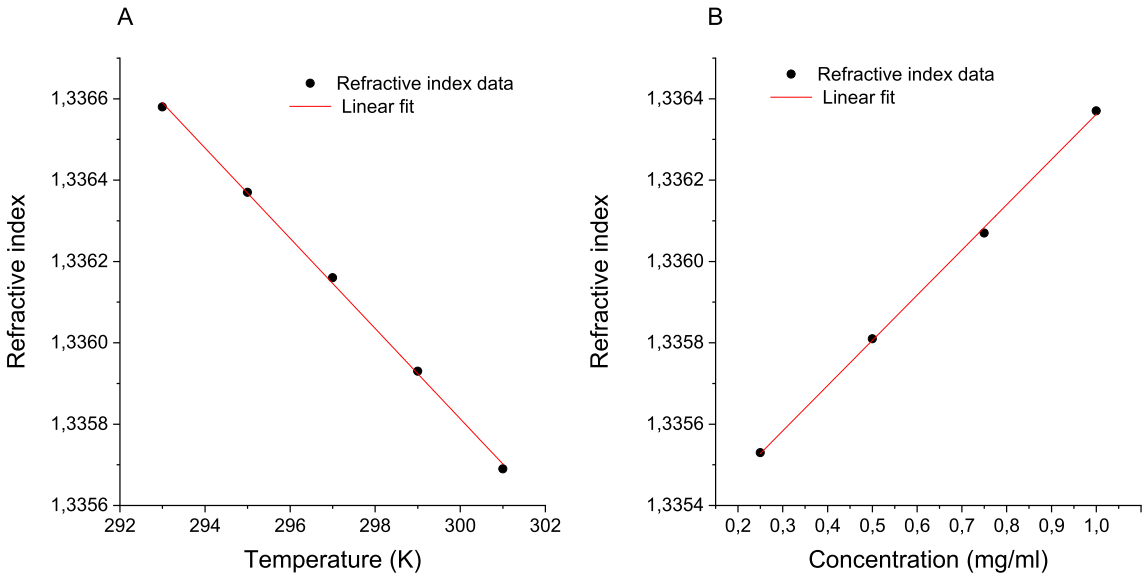

Fig. 4 Refractive index measurements as a function of the temperature (**A**) and as a function of the sample concentration (**B**) (at 22.5 °C), to LDL sample 2

The results of S_T obtained reveal different values to the coefficients from the two samples. This indicated that the absolute value of the coefficient may depend on the LDL sample characteristics, i.e., depends on the donor. Differences in the composition, structure and distribution of LDL subtractions from different individuals have been reported [30–32]. In addition, particles from different individuals may exhibit variations in oxidative levels. These oxidative stages can impose charge differences on the surface of LDL particles [13, 33]. However, it is premature from our results, to stablish a correlation between these aspects and the Soret coefficient without additional investigations.

Despite the difference in the absolute values of S_T, from the two donors, both exhibited the same sign. Considering that LDL samples have $\frac{dn}{dc} > 0$ and $\frac{dn}{dT} < 0$, the profile of the matter-lens typical result (valley-to-peak, see, e.g., Fig. 3) gives $\theta_{SL} > 0$ and (according to Eq. 10) $S_T < 0$, i.e., thermophilic behavior of the LDL particles.

4.4 S_T of LDL at physiological temperature

The same experimental approach described above was applied to investigate the behavior of LDL particles at 37.5 °C, a temperature around the physiological temperature. The LDL sample was from a new batch of preparation and called sample 3. Its absorbance spectra is presented in Fig. 5 and has the same characteristic shape, already described to LDL samples in the previous section. The coefficient α determined is given in Table 2.

Thermal- and Soret-lens results (Fig. 6) indicated the same profile of the ZS curves obtained in experiments carried out at 22.5 °C, showing that LDL particles also show a thermophilic behavior ($S_T < 0$) at physiological

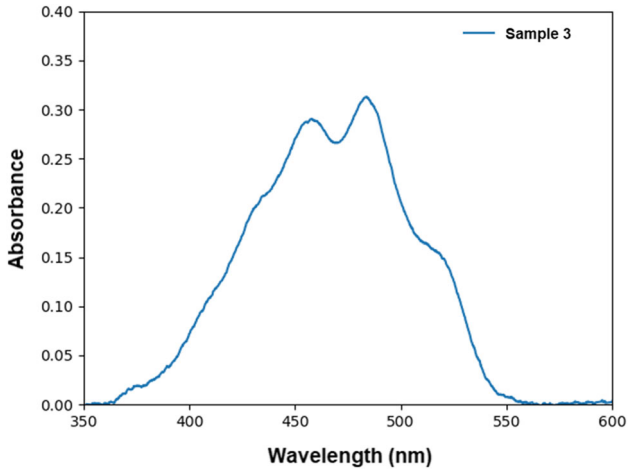

Fig. 5 Absorbance spectra in the wavelength range from 350 to 600 nm to LDL sample, measured at 37.5 °C

temperature. The θ_{TL}, θ_{SL} and S_T values are presented in Table 2.

4.5 Temperature dependence of S_T for LDL particles

Aiming to investigate S_T behavior as a function of temperature $S_T(T)$, a set of three experiments with one LDL sample, i.e., from the same donor and same batch of preparation, was performed. The S_T values were determined at 15.0, 22.5 and 37.5 °C. Since the LDL is a bioparticle, we choose the range between 15 and 37.5 °C, where the integrity of the LDL is maintained. Out of this range, the stability of the particle may be compromised. An LDL sample from the same preparation batch was used in all experiments; however, a new aliquot was used in the analyses at each temperature, to ensure the integrity of the particles. Also, to ensure a fresh sample for all measurements, the Soret experiments were optimized by reducing the number of z-positions in the Z-scan experiments.

The results of the optical experiments are shown in Figs. 7, 8 and 9. Figure 10 presents S_T as a function of temperature, in the range from 15 to 37.5 °C.

As described for many different systems, LDL showed a decrease in the absolute values of S_T, with the increase in the sample temperature. However, the signal of the Soret coefficient does not change, indicating that the same thermophilic behavior of LDL particles at the temperatures investigated.

Based on the study of some systems, Iacopini et al. [6, 34] proposed a phenomenological description for the temperature dependence of S_T, given by

$$S_T = S_T^{\infty}\left[1 - e^{(T^* - T)/T_0}\right] \tag{12}$$

where S_T^{∞} is the higher S_T value achieved at temperatures in which its values have stabilized, T^* is the

Table 2 P, α and c are the laser light incident power, the absorption coefficient and sample concentration, respectively

	P(W)	$\alpha(\mathrm{m}^{-1})$	c(mg/mL)	θ_{TL}	θ_{SL}	$dn/dT(\mathrm{K}^{-1})$	$dn/dc(\mathrm{mg/mL})^{-1}$	S_T (K^{-1})
Native LDL								
Sample 3	0.15	17.4	1.1	-0.041 ± 0.002	0.028 ± 0.003	-1.70×10^{-4}	1.15×10^{-3}	-0.09 ± 0.01

θ_{TL}, θ_{SL} and S_T are the amplitude of the thermal and matter lenses and the Soret coefficient, respectively. dn/dT is the thermal coefficient, and $\mathrm{d}n/\mathrm{d}c$ is the variation of the refractive index as a function of the sample concentration

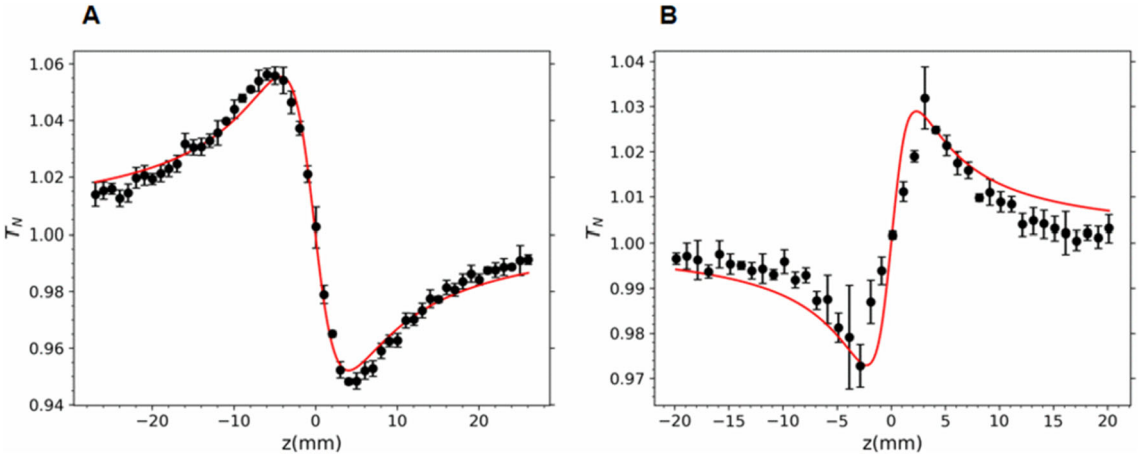

Fig. 6 Thermal- (**A**) and matter-lens (**B**) results for the LDL sample 3 studied at 37.5 °C. Symbols represent experimental data, and lines are the theoretical fittings (Eq. 11)

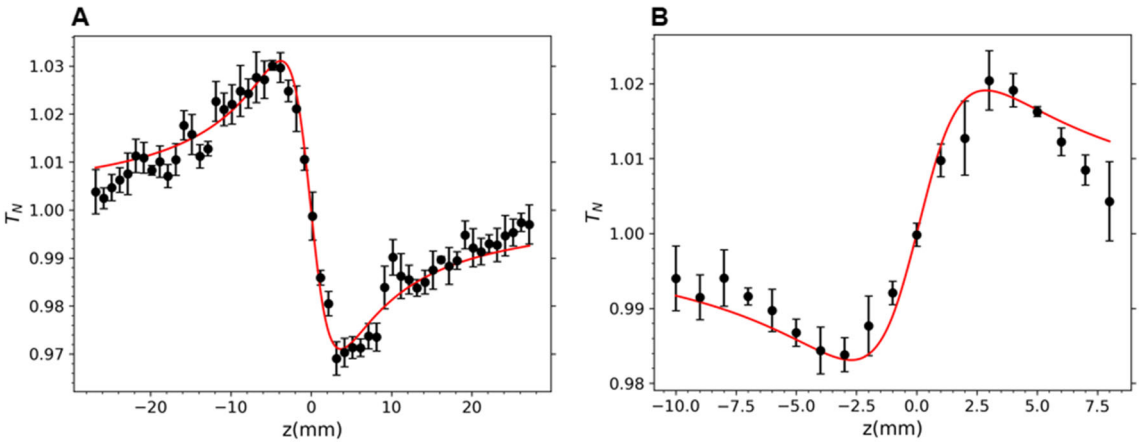

Fig. 7 Thermal- (**A**) and matter-lens (**B**) results for the LDL sample 4 studied at 15 °C. Symbols represent experimental data, and lines are the theoretical fittings (Eq. 11)

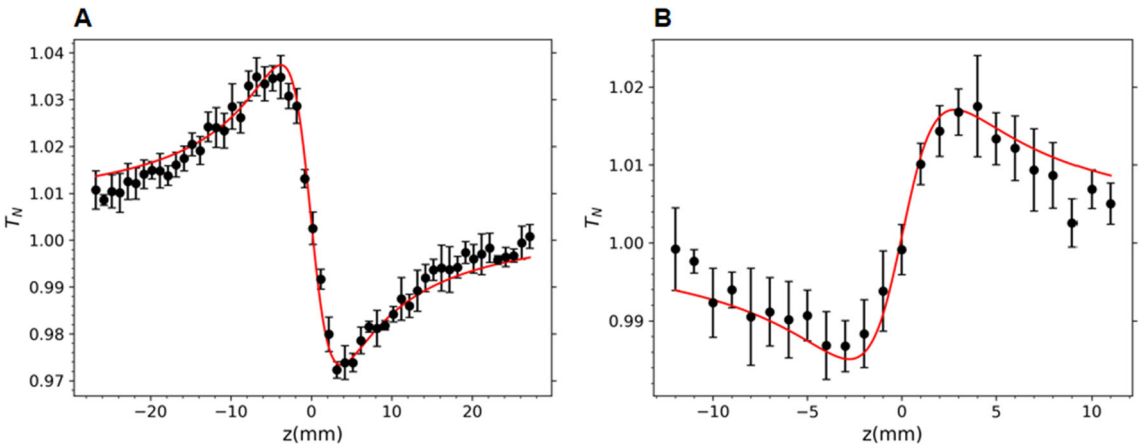

Fig. 8 Thermal- (**A**) and matter-lens (**B**) results for the LDL sample 4 studied at 22.5 °C. Symbols represent experimental data, and lines are the theoretical fittings (Eq. 11)

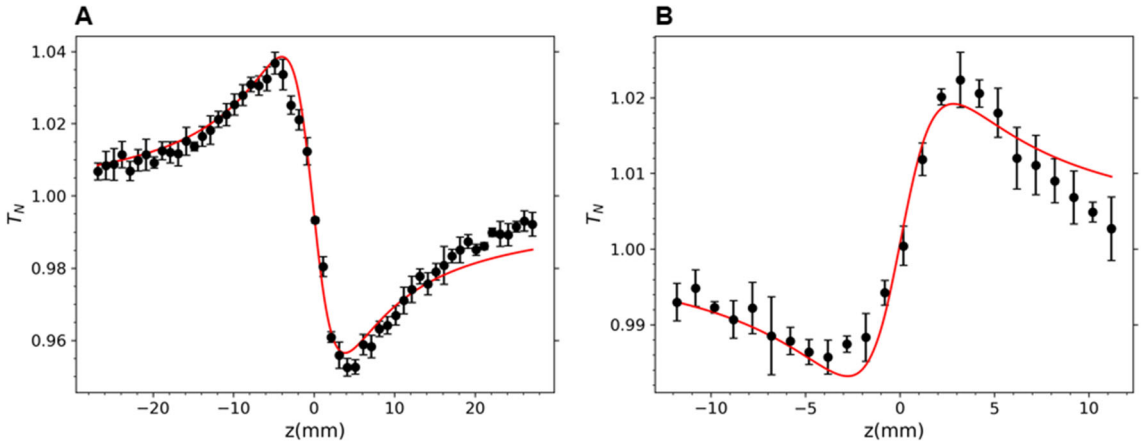

Fig. 9 Thermal- (**A**) and matter-lens (**B**) results for the LDL sample 4 studied at 37.5 °C. Symbols represent experimental data, and lines are the theoretical fittings (Eq. 11)

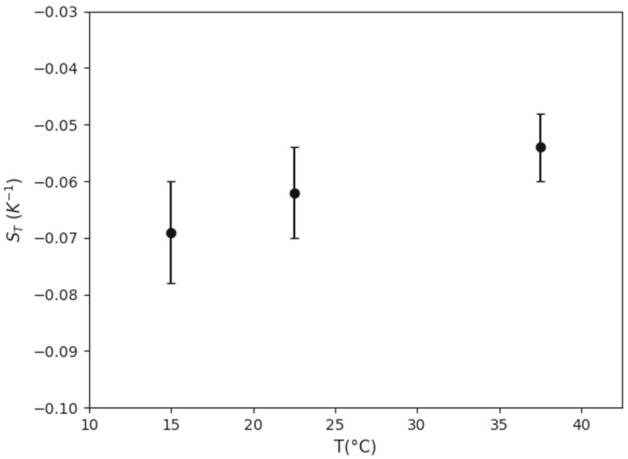

Fig. 10 Temperature dependence of S_T for LDL particles. The same LDL sample was investigated at equilibrium temperatures of 15.0, 22.5 and 37.5 °C

temperature in which the sign of S_T changes and T_0 a parameter associated with the exponential growth rate.

We tried to fit our data with Eq. (12), to obtain, at least, the order of magnitudes of the parameter proposed by Iacopini. However, due to the reduced number of experimental points in Fig. 10, the fitting is not robust, given rise to different set of parameters with equivalent values of Chi-square. So, we may just say that the dependence of $S_T$with the temperature is consistent with Eq. (12). Moreover, our results show that, unlike other colloidal systems [6, 24, 34], the LDL samples presented a slow increase in the S_T, and a non-inversion of its sign in the temperature range investigated.

The origin of the thermophilic behavior of the LDL particles, as well as its dependence on temperature, is not yet completely understood. However, we can discuss some aspects that can shine some light to this question. LDL particles have a single apolipoprotein (ApoB-100), arranged around the LDL [35]. ApoB-100 is a protein constituted by charged amino acids, such as lysins, a positively charged residue. Another characteristic of LDL particles, and the ApoB-100, is their amphipathic nature. Segrest et al. [14, 36] described ApoB-100 as a sequence of five alternating α-helix and β-sheet amphipathic domains. β-sheet rich domains probably interact directly with the lipid core through their hydrophobic faces, while predominantly α-helical domains are possibly more flexible regions of the ApoB-100, with a reversible lipid association [14]. Based on this, aspects concerning the termodiffusion of charged particles, and the role of the hydrophobic interactions' particle solvent, could play a role in the thermal behavior of the particle.

One of the first theories to describe the Soret effect in charged particles was proposed by Ruckenstein [37]. The termodiffusive phenomenon was described considering the migration of charged particles in a thermal gradient, with the result of an interfacial tension gradient [37]. According to this approach, the charged particles, under a thermal gradient, acquire a thermophoretic migration velocity (v_T) due to the interfacial tension gradient, given by

$$v_T = \frac{-l}{\eta}\frac{\mathrm{d}\gamma}{\mathrm{d}z} = \frac{-l}{\eta}\frac{\mathrm{d}\gamma}{\mathrm{d}T}\frac{\mathrm{d}T}{\mathrm{d}z} \tag{13}$$

where l is the Debye length of charged particle, η is the fluid viscosity, γ is the interfacial tension and z is the distance in the motion direction [37].

From Eq. (13), Iacopini et al. [34] proposed a relation between Soret coeficient and $\gamma\prime(T) = \frac{\mathrm{d}\gamma}{\mathrm{d}T}$, in a study of the Soret effect of lysozyme. It has been suggested that termodiffusion behavior is weakly dependent on electrostatic effects, with hydrophobic interactions playing an important role in thermodiffusion in protein solution [6, 38]. The negative values to S_T at low temperatures, the same coefficient sign we found for LDL was explained based on numerical results of γ for hydrophobic particles, which results in $\gamma\prime(T) < 0$ [34, 39]. Thus, the migration of the lysozyme to hot or cold was associated with the exposure of hydrophobic groups to the

solvent. At lower temperatures, lysozyme describes a thermophilic behavior like hydrophobic charged particles. As temperatures increase, it switches to a thermophobic behavior similar to hydrophilic charged particles. In studies with micellar systems, changes in thermophoretic migration associated with changes in interaction between hydrophobic groups and the solvent were observed [24].

In a similar way, ions present in the solution can migrate under a thermal gradient. The ions movement generates an electric field, the thermoelectric field. This phenomenon is called Seebeck effect and is due to the intrinsic Soret effect of ions [19, 40]. The Seebeck effect contribution to the Soret effect of charged particles was discussed by Eslahian et al. [21]. An expression for S_T, which considers the effects of ions and particles movement under a thermal gradient, can be written as [21, 41] follows:

$$S_T = \frac{\epsilon}{\eta T D_M}\left[\frac{\zeta^2}{12}(1+\tau+\alpha) - \zeta S T\right] \qquad (14)$$

where ϵ is the solution dielectric permittivity, τ is a parameter related to water permittivity, D_M is the mass diffusion coefficient, ζ is zeta potential, α is the thermal diffusion factor and S is the Seebeck coefficient [21, 41]. The thermoelectric field can be writing as a function of the temperature gradient by $E = \mathrm{S}\nabla T$ [19].

Unlike Eq. (12), this definition considers the influence of physical parameters such as the zeta potential (ζ), associated to extent of the electric double layer, and the Seebeck coefficient (S), associated to the thermoeletric field. Sehnem et al. [19] investigated the S_T temperature dependence of ionic ferrofluids, considering contributions from electric double layer changes and thermoeletric field action. In that work, ζ and S were measured, and the Seebeck coefficient was determined experimentally by time evolution of the thermoelectric potential in the ionic solution.

The investigation of the effect of different ions in colloidal solutions showed that distinct ions have different influences on the Soret coefficient [21, 41, 42]. Vigolo et al. [42] showed the effect of NaOH addition in micellar solutions of the anionic surfactant sodium dodecyl on the S_T of the micelles. In comparison, NaCl salt ions exhibited a weak contribution for this effect [42]. In a review paper, Niether and Wiegand [24] discussed results from biological systems subjected to thermal gradients. The effect of the temperature and concentration of the solutes, in aqueous systems, were shown to be important not only concerning the absolute value of the Soret coefficient, but also on its sign.

In the case of the LDL particles, the termophilic behavior cannot be attributed to a single characteristic of this complex structure. The ApoB-100 located around the particle is, mainly, a hydrophobic scaffold protein. On the other hand, the polar heads of the phosphatidylcholine form H bonds with the water molecules present in the plasma solution. Moreover, in the plasma, ions are present and may have crucial role in the thermodiffusion of the LDL.

The S_T values of the LDL particles measured are of the same order of magnitude of those obtained for lysozyme and SDS micelles [6, 24]. Regardless of the common thermophilic behavior, our results indicated differences in the S_T magnitude of LDL from different donors (plasma from different origins), suggesting a thermal migration influenced by specific characteristics of these particles. Since all the LDL particles investigated here were dispersed in the same medium (pH conditions and salt concentration), the ionic (Seebeck) contribution cannot explain the differences observed in the values of S_T of the LDL from different donors.

Another important point was to ensure that the thermodiffusion behavior described is due a migration of monomeric LDL, without particles aggregation in the samples. In order to this, samples 2, 3 and 4 were analyzed by DLS. The samples investigated showed a size distribution consistent with the mean LDL particles diameter reported in the literature [12]. Supplementary material can be accessed to view the DLS results.

Despite the presence of charges in LDL apolipoprotein, termodiffusion studies in protein solution indicate a non-relevant influence of this in S_T temperature dependence [6, 38]. In contrast, hydrophobic interactions between particles and solvent are suggested to be an important contribution to the $S_T(T)$ profile. Considering the amphipathic character of LDL particles, the distribution of hydrophobic/hydrophilic groups (whether or not these are exposed on the particle surface) may be considered as a contribution in the S_T dependence with temperature.

The temperature dependence of S_T was small, in the temperature range investigated, in comparison with other systems. Considering that strongest hydrophilic behavior of particles is associated to a more sensitive dependence of S_T with temperature, a more global hydrophobic behavior of LDL could be assumed. In addition, this assumed that global hydrophobic behavior of LDL would also be consistent with the negative coefficient found ($S_T < 0$), observed in the lysozyme solution.

It cannot be excluded that conformational changes in LDL may affect $S_T(T)$, since LDL particles have a core packaging phase transition, inducing changes in the overall shape of these particles. Elliptical particles at low temperatures become spherical at temperatures above the core phase transition, around 20–30 °C [43, 44].

Finally, the influence of the thermoelectric field is another interesting point. However, it is not possible to evaluate it without additional measurements, such as the zeta potential and Seebeck coefficient.

5 Conclusions

This work presents a thermodiffusive study of human LDL particles in physiological solution, in the temperature range from 15 to 37.5 °C, measuring the absolute value and sign of the Soret coefficient. The generalization of the thermal-lens model, applied to Z-scan experiments in the time scale of seconds, was employed. The thermal behavior of the LDL particles, under conditions similar to physiological environment, was shown to be thermophilic. This result may be interesting in the investigation of the plaque formation in arteries, subjected to local temperature gradients.

The previous works that addressed the diffusion of LDL particles under thermal gradients, by conditions of hyperthermia or hypothermia, employed positive value of Soret coefficient ($S_T > 0$) [15, 18]. However, our experimental results suggest negative S_T values for LDL, exhibit a thermophilic behavior. These theoretical descriptions could be revisited considering the inversion of the transport of LDL particles. For instance, the previous description for hyperthermia conditions was an LDL particle accumulation inside the arterial wall [15]. Based on our results, the increase in LDL concentration in arterial wall occurs when the heating is internal, i.e., under hypothermic conditions.

The origin of this behavior is not, still, fully understood, due to the complexity of the LDL particle. Additional experiments are necessary to investigate the different contributions to the thermophilic behavior observed.

Supplementary Information The online version contains supplementary material available at https://doi.org/10.1140/epje/s10189-023-00377-5..

Acknowledgements Authors thank André L. Sehnem and Sarah Alves for helpful discussions. This study was supported from Brazil, the National Council for Scientific and Technological Development (CNPq – 465259/2014-6), the Coordination for the Improvement of Higher Education Personnel (CAPES), the National Institute of Science and Technology Complex Fluids (INCT-Fcx) and the São Paulo Research Foundation (FAPESP – 2014/50983-3), (FAPESP – 2016/24531-3).

Author contribution statement

LOM carried out the experiments, analyzed data, participated in the design of the study and writing of the paper; DR performed technical work in the experimental setup and technical work in data acquisition and AMFN participated in the design of the study and writing of the paper.

Availability of data and materials All data generated or analyzed during this study are included in this article.

Declarations

Conflict of interest The authors declare no competing interests.

References

1. C. Soret, Surl'état d'équilibre que prend au point de vue de as concentration une dissolution saline primitivement homohéne dont deux parties sont portées à des températures différentes. Arch. Sci. Phys. Nat. **2**, 48–61 (1879)
2. R. Rusconi, L. Isa, R. Piazza, Thermal-lensing measurement of particle thermophoresis in aqueous dispersions. J. Opt. Soc. Am. B **21**, 605–615 (2004)
3. S. Duhr, D. Braun, Why molecules move along a temperature gradient. Porc. Nat. Acad. Sci. **103**, 19678–19682 (2006)
4. S.A. Putnam, D.G. Cahill, Transport of nanoscale latex spheres in a temperature gradient. Langmuir **21**, 5317–5323 (2005)
5. M. Braibanti, D. Vigolo, R. Piazza, Does thermophoretic mobility depend on particle size? Phys. Rev. Lett. **100**, 108303 (2008)
6. S. Iacopini, R. Rusconi, R. Piazza, The 'macromolecular tourist': universal temperature dependence of thermal diffusion in aqueous colloidal suspensions. Eur. Phys. J. E **19**, 59–67 (2006)
7. E. Lattuada, S. Buzzaccaro, R. Piazza, Thermophoresis in self-associating systems: probing poloxamer micellization by opto-thermal excitation. Soft Matter **15**, 2140–51 (2019)
8. R. Kita, G. Kircher, S. Wiegand, Thermally induced sign change of Soret coefficient for dilute and semidilute solutions of poly(n-isopropylacrylamide) in ethanol. J. Chem. Phys. **121**, 9140–9146 (2004)
9. R. Sugaya, B.A. Wolf, R. Kita, Thermal diffusion of dextran in aqueous solutions in the absence and the presence of urea. Biomacromolecules **7**, 435–40 (2006)
10. Y. Kishikawa, S. Wiegand, R. Kita, Temperature dependence of Soret coefficient in aqueous and nonaqueous solutions of pullulan. Biomacromolecules **11**(3), 740–747 (2010)
11. M. Bjelčić, D. Niether, S. Wiegand, Correlation between thermophoretic behavior and hydrophilicity for various alcohols. Eur. Phys. J. E **42**, 68 (2019)
12. R. Prassl, P. Laggner, Molecular structure of low density lipoprotein: current status and future challenges. Eur. Biophys. J. **38**, 145 (2008). https://doi.org/10.1007/s00249-008-0368-y
13. T. Hevonoja, M.O. Pentikäinen, M.T. Hyvönen, P.T. Kovanen, M. Ala-Korpela, Structure of low density lipoprotein (LDL) particles: basis for understanding molecular changes in modified LDL. Biochim. Biophys. Acta (BBA) Mol. Cell Biol. Lipids **1488**, 189–210 (2000)

14. J.P. Segrest, M.K. Jones, H. De Loof, N. Dashti, Structure of apolipoprotein B-100 in low density lipoproteins. J. Lipid Res. **42**, 1346–1366 (2001)
15. S. Chung, K. Vafai, Mechanobiology of low-density lipoprotein transport within an arterial wall—Impact of hyperthermia and coupling effects. J. Biomech. **47**, 137–147 (2014)
16. M. Iasielo, K. Vafai, A. Andreozzi, and N. Bianco, Proceedings of CHT-17, ICHMT International Symposium on Advances in Computational Heat Transfer, (2017)
17. M. Iasiello, K. Vafai, A. Andreozzi, N. Bianco, F. Tavakkoli, Effects of external and internal hyperthermia on LDL transport and accumulationwithin an arterial-wall in the presence of a stenosis. Ann. Biomed. Eng. **43**, 1585–1599 (2015). https://doi.org/10.1007/s10439-014-1196-0
18. M. Iasiello, K. Vafai, A. Andreozzi, N. Bianco, Low-density lipoprotein transport through an arterial wall under hyperthermia and hypertension conditions – An analytical solution. J. Biomech. **49**, 193–204 (2016)
19. A.L. Sehnem, A.M.F. Neto, R. Aquino, A.F.C. Campos, F.A. Tourinho, J. Depeyrot, Temperature dependence of the Soret coefficient of ionic colloids. Phys. Rev. E **92**, 042311 (2015)
20. M. Reichl, M. Herzog, A. Götz, D. Braun, Why charged molecules move across a temperature gradient: the role of electric fields. Phys. Rev. Lett. **112**, 198101 (2014)
21. K.A. Eslahian, A. Majee, M. Maskos, A. Wurger, Specific salt effects on thermophoresis of charged colloids. Soft Matter **10**, 1931–1936 (2014)
22. S. Alves, A. Bourdon, A.M.F. Neto, Generalization of the thermal lens model formalism to account for thermodiffusion in a single-beam Z-scan experiment: determination of the Soret coefficient. J. Opt. Soc. Am. B **20**, 713–718 (2003)
23. A.L. Sehnem, R. Aquino, A.F.C. Campos, F.A. Tourinho, J. Depeyrot, A.M. Figueiredo Neto, Thermodiffusion in positively charged magnetic colloids: influence of the particle diameter. Phys. Rev. E **89**, 032308 (2014)
24. D. Niether, S. Wiegand, Thermophoresis of biological and biocompatible compounds in aqueous solution. J. Phys. Condens. Matter **31**, 503003 (2019). https://doi.org/10.1088/1361-648X/ab421c
25. M. Sheik-Bahae, A.A. Said, E.W. Van Stryland, High sensitivity single-beam n2 measurements. Opt. Lett. **14**, 955–957 (1989)
26. A.L. Sehnem, D. Espinosa, E.S. Gonçalves, A.M. Figueiredo Neto, Thermal lens phenomenon studied by the z-scan technique: measurement of the thermal conductivity of highly absorbing colloidal solutions. Braz J Phys. **46**, 547–555 (2016). https://doi.org/10.1007/s13538-016-0434-3
27. J.F. Pedroso, Z. Lotfollahi, G. Albattarni, M.A. Schulz, A.M. Monteiro, A.L. Sehnem, M.A. Gidlund, A.M.F. Neto, M.A.N. Jardini, Influence of periodontal disease on cardiovascular markers in diabetes Mellitus patients. Sci. Rep. **9**, 16138 (2019). https://doi.org/10.1038/s41598-019-52498-7
28. A.P. de Queiroz Mello, G. Albattarni, D.H.G. Espinosa, D. Reis, A.M. Figueiredo Neto, Structural and nonlinear optical characteristics of in vitro glycation of human low-density lipoprotein, as a function of time. Brazil. J. Phys. **48**, 560–570 (2018). https://doi.org/10.1007/s13538-018-0600-x
29. R.J. Havel, H.A. Eder, J.H. Bragdon, The distribution and chemical composition of ultracentrifugally separated lipoproteins in human serum. J. Clin. Invest. **34**, 1345–1353 (1955)
30. T.D. Watson et al., Determinants of LDL subfraction distribution and concentrations in young normolipidemic subjects. Arterioscler. Thromb. **14**(6), 902–910 (1994)
31. B. Teng, G.R. Thompson, A.D. Sniderman, T.M. Forte, R.M. Krauss, P.O. Kwiterovich Jr., Composition and distribution of low density lipoprotein fractions in hyperapobetalipoproteinemia, normolipidemia, and familial hypercholesterolemia. Proc. Natl. Acad. Sci. U.S.A. **80**, 6662–6666 (1983). https://doi.org/10.1073/pnas.80.21.6662
32. D. Jakubauskas, M. Jansen, J. Lyngsø, Y. Cheng, J.S. Pedersen, M. Cárdenas, Toward reliable low-density lipoprotein ultrastructure prediction in clinical conditions: a small-angle X-ray scattering study on individuals with normal and high triglyceride serum levels. Nanomedicine **31**, 102318 (2021)
33. P. Avogaro, G.B. Bon, G. Cazzolato, Presence of a modified low density lipoprotein in humans. Arterioscler Thromb Vasc. Biol. **8**, 79–87 (1988). https://doi.org/10.1161/01.ATV.8.1.79
34. S. Iacopini, R. Piazza, Thermophoresis in protein solutions. Europhys. Lett. **63**, 247–253 (2003)
35. O.S. Olofsson, J. Boren, Apolipoprotein B: a clinically important apolipoprotein which assembles atherogenic lipoproteins and promotes the development of atherosclerosis. J. Intern. Med. **258**, 395–410 (2005). https://doi.org/10.1111/j.1365-2796.2005.01556.x
36. J.P. Segrest, M.K. Jones, V.K. Mishra, G.M. Anantharamaiah, D.W. Garber, apoB-100 has a pentapartite structure composed of three amphipathic alphahelical domains alternating with two amphipathic beta-strand domains. Detection by the computer program LOCATE. Arterioscler. Thromb. **14**, 1674–1685 (1994)
37. E. Ruckenstein, Can phoretic motions be treated as interfacial tension gradient driven phenomena? J. Colloid Interface Sci. **83**, 77–81 (1981)
38. S.A. Putnam, D.G. Cahill, G.C.L. Wong, Temperature dependence of thermodiffusion in aqueous suspensions of charged nanoparticles. Langmuir **23**, 9221–9228 (2007)
39. D.M. Huang, D. Chandler, Temperature and length scale dependence of hydrophobic effects and their possible implications for protein folding. Proc. Natl. Acad. Sci. U.S.A. **97**(15), 8324–8327 (2000)
40. B.T. Huang et al., Thermoelectricity and thermodiffusion in charged colloids. J. Chem. Phys. **143**, 054902 (2015)

41. A.L. Sehnem, A.M. Figueiredo Neto, D. Niether, S. Wiegand, Diffusiophoresis as ruling effect: influence of organic salts on thermodiffusion of iron oxide nanoparticles. Phys. Rev. E **98**, 062615 (2018). https://doi.org/10.1103/PhysRevE.98.062615
42. D. Vigolo, S. Buzzaccaro, R. Piazza, Thermophoresis and thermoelectricity in surfactant solutions. Langmuir **26**, 7792–7801 (2010). https://doi.org/10.1021/la904588s
43. V. Kumar, S.J. Butcher, K. Oorni, P. Engelhardt, J. Heikkonen, K. Kaski, M. Ala-Korpela, P.T. Kovanen, Three-dimensional cryoem reconstruction of native LDL particles To 16A resolution at physiological body temperature. PLoS ONE **6**, e18841 (2011)
44. S. Maric, T.K. Lind, J. Lyngsø, M. Cardenas, J.S. Pedersen, Modeling small-angle X-ray scattering data for low-density lipoproteins: insights into the fatty core packing and phase transition. ACS Nano **11**(1), 1080–1090 (2017)